ISSN 0029-3865

Notas de Física

CBPF-NF-005/26

Junho 2026

Alpha-decay of lanthanide isotopes: Accurate half-life evaluation for ^{146}Sm and ^{149}Sm

O.A.P. Tavares and E.L. Medeiros

Accepted for publication in Modern Physics Letters A (Nuclear Physics)

Alpha-decay of lanthanide isotopes: Accurate half-life evaluation for ^{146}Sm and ^{149}Sm

O.A.P. Tavares and E.L. Medeiros[1]

Centro Brasileiro de Pesquisas Físicas — CBPF/MCTI
Rua Dr. Xavier Sigaud 150 22290-180 Rio de Janeiro-RJ, Brazil

Abstract - A systematic analysis of α-decay half-lives of radioactive lanthanide isotopes, $T^{\alpha}_{1/2}$, has been developed which allows one to obtain an accurate and reliable $T^{\alpha}_{1/2}$-value of (103.4 ± 5.3) Ma for the extinct ^{146}Sm isotope, and to predict a $T^{\alpha}_{1/2}$-value of $(1.8 \pm 0.2) \times 10^{18}$ a for the yet unknown alpha radioactivity of ^{149}Sm isotope.

Keywords: Alpha-decay; lanthanide isotopes; half-life predictions; ^{146}Sm; ^{149}Sm; semiempirical method.

PACS Numbers: 23.60.+e, 27.60.+j, 27.70.+q, 91.80.Hj, 93.85.Np

A new, semiempirical method has been proposed to half-life evaluation of alpha-radioactive isotopes based on a linear correlation of decimal log of the measured half-lives with total area, $\mathcal{A}_{\rm T}$, comprised by the potential barrier curve and the Q-value for decay covering the region limited by the returning points. Such a method, which we shall call COMEVIA, was recently successfully introduced when we were analysing cases of exotic radioactivity [1]. Here, COMEVIA is being applied to alpha-decay cases of lanthanide isotopes.

The main motivation to undertake the present study was to obtain an accurate half-life value, $T^{\alpha}_{1/2}$, of the extinct, long-lived ^{146}Sm isotope to be used as a reliable chronometer for the early Solar System via the decay system ^{146}Sm-^{142}Nd [2–4]. Indeed, persistent differences, sometimes large ones, there still exist among both measured and calculated $T^{\alpha}_{1/2}$-values for ^{146}Sm [4–7]. Therefore, an accurate determination of half-life for ^{146}Sm is of utmost importance in dating of meteoritic samples by means of the pure α decaying $^{146}\mathrm{Sm} \rightarrow {}^{142}$Nd isotopic chronometer as well as in many geochronological and astrophysical applications [8].

In addition, the COMEVIA method makes it possible to predict an alpha-decay half-life value for ^{149}Sm isotope that was not yet measured at all.

Basically, the present method to obtain accurate predictions of α-decay half-lives consists of

[1] Corresponding author: *emildelimamedeiros@gmail.com*

developing a systematic statistical analysis of known experimental data of a selected region of parent nuclei, thus allowing to extract some doubtful or unknown half-life values of nuclei located in that region. Since we are investigating the α-radioactivity of ^{146}Sm and ^{149}Sm, we have considered in the present analysis the region of lanthanide radioisotopes.

For this region of α-active isotopes the classical frequency of assaults of alpha particles to penetrate the potential barrier does not vary significantly ($\sim (0.92\text{–}1.71) \times 10^{21}\,\mathrm{s}^{-1}$), and the width of the overlapping barrier is practically constant as well (~ 3.17 fm, see below). Therefore, the α-decay half-life, $T_{1/2}^{\alpha}$ (or $\tau = \log_{10} T_{1/2}^{\alpha}$), should depend essentially on the extension and height of the separation barrier. These two variables are to a great extent proportional to $(Z-2)/Q_{\alpha}$ and $(Z-2)/(A-4)^{1/3}$, respectively, so that $T_{1/2}^{\alpha}$ should increase with the quantity $z = (Z-2)^2/[Q_{\alpha} \cdot (A-4)^{1/3}]$ (Z and A represent the atomic and mass numbers, respectively, of the α-emitter nuclide; see Fig. 1). Since the quantity z on the abscissa takes into account neither centrifugal effects nor nuclear deformation, the trend shown in Fig. 1 is approximate, indicating only that there may be a simple and precise linear relationship between $T_{1/2}^{\alpha}$ and $\mathcal{A}_{\mathsf{T}}$, this latter quantity being defined above (1st paragraph). Indeed, this task has been accomplished by the authors recently [1].

To start with, the potential energy barrier should describe the two adjacent regions through which the alpha decaying process occurs, namely, the overlapping and separation regions. For the first one we have assumed a power function of $s-a$ ($a \leq s \leq c$) (s is the separation between the centers of the nascent fragments) where $a = R_{\mathsf{P}} - R_{\alpha}$ is the inner turning point, and $c = R_{\mathsf{D}} + R_{\alpha}$ is the configuration of contact of the preformed α particle with the residual (daughter) nucleus (see Fig. 2):

$$V_{\mathrm{ov}}(s) = Q + (V_c - Q)\left(\frac{s-a}{c-a}\right)^q,\ q \geq 1\,, \tag{1}$$

and the total potential energy at contact configuration, V_c, is given by the Coulomb plus centrifugal energies, *viz.*

$$V_c = \frac{2Z_{\mathsf{D}} \cdot e^2}{c} + \frac{\ell(\ell+1)\hbar^2}{2\mu_0 c^2}\,. \tag{2}$$

Here, $e^2 = 1.43996444$ MeV$\cdot$fm is the square of the electronic elementary charge, ℓ is the mutual orbital angular momentum resulting from the rotation of the decaying product nuclei around their common center of mass, $\hbar = h/(2\pi) = 6.582119 \times 10^{-22}$ MeV$\cdot$s is the Planck's constant, μ_0 is the effective reduced mass of the already formed fragments through the separation region ($c \leq s \leq b$), b is the outer turning point, R_{P}, R_{D}, and R_{α} denote the radius of the parent (emitter) nucleus, the daughter nucleus and the alpha-particle, respectively (see Appendix), Q is the total disintegration energy, *i.e.*, the Q-value of the alpha decaying process, and Z_{D} is the atomic number of the produced nucleus (the quantities Q and μ_0 are described in the Appendix).

In the separation region ($c \leq s \leq b$) (see Fig. 2) the potential energy is formed by the Coulomb plus centrifugal contributions, *i.e.*

$$V_{\rm sp}(s) = \frac{2Z_{\rm D}e^2}{s} + \frac{\ell(\ell+1)\hbar^2}{2\mu_0 s^2} \ , \tag{3}$$

and b, the outer turning point, is obtained from the condition $V_{\rm sp}(b) = Q$. When $\ell = 0$, $b = 2Z_{\rm D}e^2/Q$.

By introducing the dimensionless quantities

$$x = \frac{\ell(\ell+1)\hbar^2}{2\mu_0 c^2 Q} \ , \ u = \frac{cQ}{2Z_{\rm D}e^2} \ , \text{ and } y = \frac{1+u^2x}{u} \tag{4}$$

we have

$$V_{\rm ov}(s) = Q\left[1 + \left(\frac{1-u}{u} + x\right)\left(\frac{s-a}{c-a}\right)^q\right], \ V_{\rm sp}(s) = cQ\left(\frac{1}{us} + \frac{cx}{s^2}\right). \tag{5}$$

Therefore, the total area under the potential barrier curve and above the Q-value (Fig. 2) is calculated as

$$\mathcal{A}_{\rm T} = \mathcal{A}_{\rm ov}(s) + \mathcal{A}_{\rm sp}(s) = \int_a^c \left[V_{\rm ov}(s) - Q\right] {\rm d}s + \int_c^b \left[V_{\rm sp}(s) - Q\right] {\rm d}s \, . \tag{6}$$

In the present calculations we have expressed lengths in fm, masses in u, and energies in MeV, so that the areas are given in MeV$\cdot$ fm. When $\ell \neq 0$ the condition $V_{\rm sp}(b) = Q$ leads to the solution $b = c/(2u) \cdot (1 + \sqrt{1+4u^2x})$. It turns out that for the α-transitions of lanthanide isotopes the values for the quantity $u^2x \approx 0.65Q\ell(\ell+1)/Z_{\rm D}^2$ are such that $0 \leq u^2x \lesssim 0.02$. Therefore the term $1 + \sqrt{1+4u^2x}$ can be replaced by $2(1+u^2x)$ and, finally, $b = cy$ (cf. eq. (4)).

After straightforward calculation it results

$$\mathcal{A}_{\rm T} = Q\left\{\left(\frac{1-u}{u} + x\right)\frac{(c-a)}{q+1} + c\left[\frac{\ln y}{u} + x\left(1 - \frac{1}{y}\right) + (1-y)\right]\right\}. \tag{7}$$

As regards the exponent q which appears in (1) and (7), we have found out that an increasing, rather linear dependence of $\tau = \log T_{1/2}$ upon $\mathcal{A}_{\rm T}$ was evidenced when parameter q was put equal to $1/u$ when we studied cases of exotic radioactivity [1]. The same happens in the present analysis of α-decay of lanthanide isotopes.

Proceeding in the same way here as before, formula (7) transforms to

$$\mathcal{A}_{\rm T}(\ell \neq 0) = Q\left\{\frac{[1-u(1-x)](c-a)}{1+u} + c\left[\frac{\ln y}{u} + x\left(1 - \frac{1}{y}\right) + (1-y)\right]\right\} \tag{8}$$

$$\mathcal{A}_{\rm T}(\ell = 0) = Q\left\{\frac{1-u}{1+u}(c-a) + c\left[1 - \frac{1+\ln u}{u}\right]\right\}. \tag{9}$$

Figure 2 shows three examples of α-decay of lanthanide isotopes, where it is clearly seen an increasing of the shaded areas with increasing of the half-life. Looking at parts a) and c) in Fig. 2, an increasing by 1.86 times in the potential-barrier area implies a variation by twenty-seven orders of magnitude in the half-life.

By expressing $T^{\alpha}_{1/2}$ in annum (a) and plotting τ *vs* $\mathcal{A}_{\rm T}$, we have analysed fifty cases of alpha transitions in the region of lanthanides (obviously excluding ^{146}Sm), grouping the $T^{\alpha}_{1/2}$-data into two sets of experimental data according to the half-life values. The first one comprises isotopes of 10^{-5} a $\lesssim T^{\alpha}_{1/2} \lesssim 10^{19}$ a (Fig. 3), and the other one those of 10^{-9} a $\lesssim T^{\alpha}_{1/2} \lesssim 10^{-2}$ a (Fig. 4), covering a total of twenty-eight orders of magnitude in $T^{\alpha}_{1/2}$.

In Fig. 3 the straight line is the result of the weighted least squares fit through the points, where nineteen of them, identified by numbers near the black circles, represent the experimental data best adjusted to the straight line

$$\tau_{\rm c} = (0.2342 \pm 0.0007)\mathcal{A}_{\rm T} - (44.206 \pm 0.141),\ 170 < \mathcal{A}_{\rm T} < 270 \tag{10}$$

(standard deviation $\sigma = 0.087$, linear correlation coefficient $r = 0.9985$).

In Table 1 are reported the nineteen decay cases plotted as black circles in Fig. 3, plus the decay data for ^{146,149,150}Sm isotopes. It is seen in Table 1 that among the twenty α-decay measured cases seventeen of them show the ratio $T^{\sf calc}_{1/2}/T^{\sf exper}_{1/2}$ (or its inverse) in the range $\sim$ 1–2, thus indicating good reproducibility of the experimental data by the COMEVIA calculation routine.

An important result that can be useful in investigations on chronology of the early Solar System is highlighted in Fig. 3 by a red square, which indicates at $\mathcal{A}_{\rm T} = 222.975$ MeV$\cdot$ fm the value (103.4$\pm$5.3) Ma for the half-life of ^{146}Sm. This calculated result, obtained by the present COMEVIA method, compares quite well with the measured values (102.6 $\pm$ 4.8) Ma [12], (103.1 $\pm$ 4.5) Ma [13], (102 $\pm$ 9) Ma [14] as well as the calculated ones (103.7 $\pm$ 2.4) Ma [19] and (102.5 $\pm$ 1.9) Ma [20].

Furthermore, Table 1 allows one to predict new half-life values for two α-emitter isotopes not yet measured. For ^{149}Sm isotope the value $T^{\alpha}_{1/2} = (1.8 \pm 0.2) \times 10^{18}$ a has been obtained, which is feasible to be attained by the current experimental techniques. However, for ^{150}Sm isotope, with a predicted value of $T^{\alpha}_{1/2} = (6.0 \pm 0.8) \times 10^{21}$ a it would be at present very difficult to detect any α-activity. The black squares in Fig. 3 represent those $T_{1/2}$-data that were eliminated in four sequential runs in the weighted least squares analysis (these last ones are listed in Table 2).

Table 3 shows for five Samarium isotopes an intercomparison of calculated $\tau_{\sf c}$-values by four parameterizations with the experimental data. The predictive power of the present COMEVIA method is demonstrated by observing the cases for ^{146,147}Sm. Good agreement is also seen between

the result of this work and Ren's prediction for ^{149}Sm, and also the present estimate and that by Duarte *et al.* [16] for ^{148}Sm. The best estimates of τ_{c}-value for ^{148}Sm are those given by Denisov [17] and Ren *et al.* [18]. However, large differences exist in τ_{c}-values in the case for ^{150}Sm isotope.

In Fig. 4 is depicted the group of twenty-one lanthanide alpha emitter isotopes of lowest half-life value. Again, the weighted least squares fit was applied to the experimental data, thus obtaining the straight line

$$\tau_{\mathsf{c}} = (0.2170 \pm 0.0018)\mathcal{A}_{\mathrm{T}} - (40.090 \pm 0.285),\ 144 < \mathcal{A}_{\mathrm{T}} < 178 \tag{11}$$

(standard deviation $\sigma = 0.069$, linear correlation coefficient $r = 0.9970$), near to which are located twenty points (black triangles) of isotopes identified by numbers. This time just one α-decay case, $^{157}\mathrm{Lu}^{m} \rightarrow ^{153}\mathrm{Tm}$ (black square), is seen slightly offset from the weighted linear fit (see Table 2). For all the twenty experimental τ_{e}-values of Sm isotopes depicted in Fig. 4 (black triangles) the ratio $T_{1/2}^{\mathsf{calc}}/T_{1/2}^{\mathsf{exper}}$ (or its inverse) results to be $\lesssim 2$, which corroborates the good predictive power of the COMEVIA method.

The present analysis of all experimental $T_{1/2}^{\alpha}$-data of lanthanide isotopes indicates that 70% of cases have their $T_{1/2}^{\alpha}$-values reproduced by a factor < 2, 8% within a factor between 2 and 3, and 22% by a factor > 3.

The reliability of the present COMEVIA method, which enabled us to estimate doubtful and unknown α-decay half-lives of radionuclides belonging to the lanthanide group of known $T_{1/2}^{\alpha}$-values, can be appreciated by looking at Fig. 5. This figure shows $\Delta\tau = \tau_{\mathsf{c}} - \tau_{\mathsf{e}}$ distributions resulting from three different approaches to obtain $\Delta\tau$-value applied to the set of lanthanide isotopes, *viz.*, i) improved Royer formula [19, 20] to include centrifugal potential and blocking effects of unpaired nucleons (Deng *et al.* [21], blue histogram); ii) use of α-particle preformation probability by Xu and Ren [22] who introduced only one adjustable parameter in the harmonic oscillator potential model by Bayrak [23] (Zhu *et al.* [10], red histogram); and iii) the present COMEVIA approach that fits known $T_{1/2}^{\alpha}$-data to straight lines (this work, histogram delimiting the grey-shaded region). The intercomparison between these histograms in Fig. 5 makes it clear about the suitability of the present method in reproducing the measured data in an acceptable way too. The 22% of measured cases of half-lives not reproduced satisfactorily in the present analysis ($|\Delta\tau| \gtrsim 0.48$, see Table 2) may be ascribed to combined uncertainties that exist in nuclear mass and radius, angular momentum, also perhaps to uncertainties in the experimental determination of the partial $T_{1/2}^{\alpha}$-values, and to causes more difficult to be identified.

To conclude, COMEVIA approach described here and applied to α-decay half-lives of lanthanide isotopes proved to be adequate in indicating of a reliable value for the half-life of ^{146}Sm [(103.4 $\pm$

5.3) Ma], and also to predict ^{149}Sm as a problable, new alpha emitter nuclide of half-life $(1.8 \pm 0.2) \times 10^{18}$ a. The present approach can certainly be used to other groups of isotopes of the region of intermediate-mass ($72 \leq Z \leq 83$), actinide, and superheavy nuclei as well in order to elucidate eventually cases of doubtful or even unknown half-life values. We anticipate results confirmed.

Appendix

The application of COMEVIA method in the routine calculation to obtain $\mathcal{A}_{\rm T}$-values for α-decay cases of lanthanide isotopes analysed in this work requires knowledge of three basic quantities, *viz.*, i) nuclear mass, ii) nuclear radius, and iii) angular momentum associated with the α-transition.

Values of both quantities Q and μ_0 have been derived from the nuclear (rather than atomic) mass-values of the participating nuclides, namely

$$Q = m_{\mathsf{P}} - (m_{\mathsf{D}} + m_\alpha), \quad \mu_0 = \frac{m_{\mathsf{D}} \cdot m_\alpha}{m_{\mathsf{D}} + m_\alpha}, \tag{A1}$$

where the m's are given by

$$m_i = A_i - Z_i \cdot m_{\mathsf{e}} + \frac{\Delta M_i + k \cdot Z_i^\zeta}{F}, \;\; i = \mathsf{P},\, \mathsf{D}, \tag{A2}$$

in which $F = 931.4940038$ MeV/u is the mass-energy conversion factor, $m_{\mathsf{e}} = 0.5485799 \times 10^{-3}$ u is the electron rest mass, $m_\alpha = 4.00150617$ u, and ΔM is the atomic mass-excess values as tabulated by Wang *et al.* [24]. The quantity $k \cdot Z_i^\zeta$ represents the total binding energy of the Z_i electrons in the atom, where the values

$$k_1 = 8.7 \times 10^{-6} \text{ MeV and } \zeta_1 = 2.517 \text{ for } Z \geq 60 \text{ and}$$

$$k_2 = 13.6 \times 10^{-6} \text{ MeV and } \zeta_2 = 2.408 \text{ for } Z < 60 \tag{A3}$$

have been obtained from data reported by Huang *et al.* [25]. Thus, the Q-value for decay is calculated as

$$Q = \Delta M_{\mathsf{P}} - \Delta M_{\mathsf{D}} - 2.424916 + S \text{ MeV}, \tag{A4}$$

$$S = 10^{-6} \left[k(Z_{\mathsf{P}}^\zeta - Z_{\mathsf{D}}^\zeta) - 72.1804 \right] \text{MeV}. \tag{A5}$$

S represents the effect of the screening to the nucleus caused by the surrounding electrons.

The nuclear-radius values, R_i ($i = \mathsf{P}, \mathsf{D}$), have been evaluated following the finite range droplet model (FRDM) of atomic nuclei as described by Möller *et al.* [26], where the spherical approximation for the nuclear volume has been adopted (see also [27]). This nuclear radius parametrization has

been updated by Möller *et al.* [28], who took into account more accurate experimental ground-state nuclear mass data. Accordingly, the expressions that enable to calculate the average equivalent root-mean-square radius-values of the proton and neutron density distributions are read as

$$R_i = \overline{Q}_{Z,A} = \frac{Z}{A}\,Q_{\rm p} + \left(1 - \frac{Z}{A}\right)Q_{\rm n},\; i = \mathsf{P}, \mathsf{D}, \tag{A6}$$

where the equivalent proton and neutron radii Q_j (j = p,n) are obtained from

$$Q_j = R_j\left(1 + \frac{5}{2R_j^2}\right). \tag{A7}$$

Here, R_j denotes the sharp radii for proton and neutron density distributions, the value of which are given by

$$R_{\rm p} = r(1+\bar{\epsilon})\left[1 - \frac{2}{3}\left(1 - \frac{Z}{A}\right)\left(1 - \frac{2Z}{A} - \bar{\delta}\right)\right]\cdot A^{1/3} \text{ and} \tag{A8}$$

$$R_{\rm n} = r(1+\bar{\epsilon})\left[1 + \frac{2Z}{3A}\left(1 - \frac{2Z}{A} - \bar{\delta}\right)\right]\cdot A^{1/3} \tag{A9}$$

with $r = 1.16$ fm, and the values for the quantities $\bar{\epsilon}$ and $\bar{\delta}$ are given by [28]

$$\bar{\epsilon} = 0.854167\exp(-0.988A^{1/3}) - \frac{0.1896936}{A^{1/3}} + 0.2229167\bar{\delta}^2 + 0.0031034\frac{Z^2}{A^{4/3}} \text{ and} \tag{A10}$$

$$\bar{\delta} = \frac{1 - \frac{2Z}{A} + 0.0048626\frac{Z}{A^{2/3}}}{1 + 2.5304666\frac{1}{A^{1/3}}}. \tag{A11}$$

In cases where quadrupole deformation of parent and/or daughter nuclei should be considered, a small correction on R_i-values given by (A6) has been introduced using the factor

$$\sqrt{1 + \frac{5\beta_2^2}{4\pi}} \tag{A12}$$

as described in [29] (β_2 is the quadrupole deformation parameter, the values of which have been taken from [28].

Concerning the alpha-particle radius, it has been adopted the value $R_\alpha = (1.62 \pm 0.01)$ fm, in accordance to the α-particle radius-value derived from the charge density distribution measured by Sick *et al*. [30] in electron scattering experiments on ^{4}He target. Excellent reproducibility of alpha-decay half-life data was attained using the above mentioned R_α-value in a systematic analysis of a large number (more than three hundred cases) of masured $T^\alpha_{1/2}$-value covering the mass-number interval $106 \leq A \leq 264$ [31].

Finally, ℓ-values have been obtained from tabulated data on nuclear spin ($\boldsymbol{J}$) and parity ($\boldsymbol{\pi}$) compiled by Kondev *et al.* [9], by applying to them the usual conservation laws $\boldsymbol{J}_\mathsf{P} = \boldsymbol{J}_\mathsf{D} + \boldsymbol{\ell}$ and $\pi_\mathsf{P} = \pi_\mathsf{D}\cdot(-1)^\ell$.

References

[1] O.A.P. Tavares and E.L. Medeiros, Cluster radioactivity of actinide nuclei by the emission of Ne, Mg and Si isotopes: A semiempirical analysis of the half-lives. *Int. J. Mod. Phys. E* **34**, (2025) 2550011.

[2] N.E. Marks, L.E. Borg, I.D. Hutcheon, B. Jacobsen, R.N. Clayton, Samarium-neodymium chronology and rubidium-strontium systematics of an Allende calcium-aluminum-rich-inclusion with implications for ^{146}Sm half-life. *Earth Planet. Sci. Lett.* **405**, (2014) 15.

[3] I.M. Villa, N.E. Holden, A. Possolo, R.B. Ickert, D.B. Hibbert, P.R. Renne, IUPAC-IUGS recommendation on the half-lives of ^{147}Sm and ^{146}Sm. *Geochim. Cosmochim. Acta* **285**, (2020) 70.

[4] S. Tang, Y. Qiam, and W. Lin, Examining evidence for a shorter ^{146}Sm$-^{142}$Nd chronology in the early Solar System. *Phys. Rev. C* **111**, (2025) L052801.

[5] W. Kutschera, R. Dressler, J. Lachner *et al.*, On some unsetled half-lives of AMA radionuclides. *Nucl. Inst. Methods Phys. Res. B* **566**, (2025) 165802.

[6] O.A.P. Tavares and M.L. Terranova, A semiempirical evaluation of half-life of ^{146}Sm isotope. *Mod. Phys. Lett. A* **38**, (2023) 2350115.

[7] Yi Wu, Ruijia Li, Chang Xu, Calibration of α-decay half-life of ^{146}Sm for the chronology of early solar system. *Phys. Lett. B* **872**, (2026) 140113.

[8] N.M. Chiera, P. Sprung, Y. Amelin, R. Dressler, D. Schumann, and Z. Talip, The ^{146}Sm half-life re-measured: Consolidating the chronometer for events in the early Solar System. *Nature Sci. Rep.* **14**, (2024) 17436.

[9] F.G. Kondev, M. Wang, W.J. Huang, S. Naimi, G. Audi, The NUBASE 2020 evaluation of nuclear physics properties. *Chin. Phys. C* **45**, (2021) 030001.

[10] X.-Y. Zhu, S. Luo, W. Gao *et al.*, An improved simple model for α decay half-lives. *Chin. Phys. C* **48**, (2024) 074102.

[11] M. Nurmia, G. Graeffe, K. Valli, J. Aaltonen, Alpha Activity of Sm-146. University of Helsinki (1964); *Ann. Acad. Sci. Fennicae A* **6**, (1964) 148.

[12] A.M. Friedman, J. Milsted, D. Metta *et al.*, Alpha decay half-lives of ^{148}Gd, ^{150}Gd and ^{146}Sm. *Radiochim. Acta* **5**, (1966) 192.

[13] F. Meissner, W.-D. Schmidt-Ott, and L. Ziegler, Half-life and α-ray energy of ^{146}Sm. *Z. Phys. A* **327**, (1987) 171.

[14] L. Fang, P. Frossard, M. Boyer, A. Bouvier, J.-A. Barrat, M. Chaussidon, F. Moynier, Half-life and initial Solar System abundance of ^{146}Sm determined from the oldest andesitic meteorite. *Proc. Natl. Acad. Sci. USA* **119**, (2022) e212093319.

[15] A.M. Friedman, J. Milsted, and A.L. Harkness, α-decay half-lives of ^{148}Gd, ^{150}Gd, and ^{146}Sm. *Bull. Amer. Phys. Soc. Ser. II* **8**, (1963) 525.

[16] S.B. Duarte, O.A.P. Tavares, F.Guzmán *et al.*, Half-lives for proton emission, alpha decay, cluster radioactivity, and cold fission processes calculated in a unified theoretical framework. *At. Data Nucl. Data Tables* **80**, (2002) 235.

[17] V.Yu. Denisov, Alpha-decay half-lives and alpha-capture cross-sections. *At. Data Nucl. Data Tables* **161**, (2025) 101684.

[18] K. Ren, P. Ma, M. Hu, J. Tian, Unified Royer law revision for α-decay half-lives. *Chin. Phys. C* **50** (2026) 024106.

[19] G Royer, Alpha emission and spontaneous fission through quasi-molecular shapes. *J. Phys. G: Nucl. Part. Phys.* **26**, (2000) 1149.

[20] G. Royer, Analytic expressions for alpha-decay half lives and potential barriers. *Nucl. Phys. A* **848**, (2010) 279.

[21] J.G. Deng, H.E. Zhang, and G. Royer, Improved empirical formula for α-decay half-lives. *Phys. Rev. C* **101**, (2020) 034307.

[22] C. Xu and Z. Ren, Favored α-decays of medium mass nuclei in density-dependent cluster model. *Nucl. Phys. A* **760**, (2005) 303.

[23] O. Bayrak, A new simple model for the α-decay. *J. Phys. G: Nucl. Part. Phys.* **47**, (2020) 025102.

[24] M. Wang, W.J. Huang, F.G. Kondev, G. Audi and S. Naimi, The AME2020 atomic mass evaluation (II). Tables, graphs and references. *Chin. Phys. C* **45**, (2021) 030003.

[25] K.-N. Huang, M. Aoyagi, M.H. Chen, B. Crasemann and H. Mark, Neutral-atom electron binding energies from relaxed-orbital relativistic Hartree-Fock-Slater calculations $2 \leq Z \leq 166$. *Atomic Data Nucl. Data Tables* **18**, (1976), 243.

[26] P. Möller, J.R. Nix, W.D. Myers, W.J. Swiatecki, Nuclear ground-state masses and deformations. *Atomic Data Nucl. Data Tables* **59**, (1995), 185.

[27] W. D. Myers, *Droplet Model of Atomic Nuclei*. Plenum, New York (1977).

[28] P. Möller, A.J. Sierk, T. Ichikawa, H. Sagawa. Nuclear ground-state masses and deformations: FRDM (2012). *Atomic Data Nucl. Data Tables* **109–110**, (2016) 1.

[29] W.H. Seif and Hesham Mansour, Systematics of nucleon density distributions and neutron skin of nuclei. *Int. J. Mod. Phys. E* **24**, (2015) 1550083.

[30] I. Sick, J.S. McCarthy, R.R. Whitney, Charge density of ^{4}He, *Phys. Lett. B* **64**, (1976) 33.

[31] E.L. Medeiros, M.M.N. Rodrigues, S.B. Duarte, O.A.P. Tavares, Systematics of alpha-decay half-life: new evaluation for alpha-emitter nuclides. *J. Phys. G: Nucl. Part. Phys.* **32**, (2006) B23.

Table 1 - Calculated (or predicted) alpha-decay half-lives, $T_{1/2}^{\mathsf{calc}}$, compared with experimental data, $T_{1/2}^{\mathsf{exper}}$, for alpha-transitions of lanthanide isotopes in cases where $1/3 \leq T_{1/2}^{\mathsf{calc}}/T_{1/2}^{\mathsf{exper}} \leq 3$.

Decay case	Q_α (MeV)	ℓ	$\mathcal{A}_{\mathsf{T}}$ [MeV·fm]	$\tau = \log_{10} T_{1/2}^{\alpha}$ [a]		$T_{1/2}^{\mathsf{calc}}/T_{1/2}^{\mathsf{exper}}$
				τ_{e} [a]	τ_{c} [b]	
^{144}Nd $\rightarrow$ ^{140}Ce	1.92149	0	252.278	15.360	14.877	0.33
^{145}Pm $\rightarrow$ ^{141}Pr	2.34329	0	229.489	9.801	9.540	0.55
^{146}Sm $\rightarrow$ ^{142}Nd	2.55108	0	222.975	8.017 [c]	8.015	0.99
^{147}Sm $\rightarrow$ ^{143}Nd	2.33365	0	235.918	11.028	11.046	1.04
^{148}Sm $\rightarrow$ ^{144}Nd	2.00935	0	258.251	15.806	16.276	2.95
^{149}Sm $\rightarrow$ ^{145}Nd	1.89349	0	266.728	——	18.262	——
^{150}Sm $\rightarrow$ ^{146}Nd	1.67270	0	281.742	——	21.778	——
^{147}Eu $\rightarrow$ ^{143}Pm	3.01400	0	204.169	3.477	3.610	1.36
^{148}Eu $\rightarrow$ ^{144}Pm	2.71658	0	219.161	7.201	7.121	0.83
^{151}Eu $\rightarrow$ ^{147}Pm	1.98683	2	268.953	18.665	18.783	1.31
^{148}Gd $\rightarrow$ ^{144}Sm	3.29472	0	196.504	1.853	1.815	0.92
^{149}Gd $\rightarrow$ ^{145}Sm	3.12274	0	204.071	3.771	3.587	0.65
^{152}Gd $\rightarrow$ ^{148}Sm	2.22727	0	248.833	14.033	14.071	1.09
^{151}Tb $\rightarrow$ ^{147}Eu	3.52015	2	194.893	1.325	1.438	1.30
^{152}Dy $\rightarrow$ ^{148}Gd	3.75111	0	187.006	−0.566	−0.409	1.43
^{153}Dy $\rightarrow$ ^{149}Gd	3.58363	0	193.121	0.890	1.023	1.36
^{153}Ho $\rightarrow$ ^{149}Tb	4.07679	0	179.482	−2.127	−2.171	0.90
^{154}Er $\rightarrow$ ^{150}Dy	4.30546	0	176.149	−2.821	−2.952	0.74
^{155}Er $\rightarrow$ ^{151}Dy	4.14403	0	181.301	−1.339	−1.745	0.39
^{155}Tm $\rightarrow$ ^{151}Ho	4.59822	0	170.787	−4.084	−4.208	0.75
^{156}Tm $\rightarrow$ ^{152}Ho	4.37162	0	177.809	−2.382	−2.563	0.66
^{156}Yb $\rightarrow$ ^{152}Er	4.83667	0	167.635	−5.082	−4.946	1.37

[a] Data taken from Refs. [9, 10].

[b] Calculated values in the present work.

[c] Weighted average from six measurements [8, 11–15].

Table 2 - The same as in Table 1 for cases of $T_{1/2}^{\mathsf{calc}} / T_{1/2}^{\mathsf{exper}} > 3$ or $< 1/3$.

		Decay case	Q_α [MeV]	ℓ	$\mathcal{A}_\mathsf{T}$ [MeV·fm]	$\tau = \log_{10} T_{1/2}^{\alpha}$ [a]		$\frac{T_{1/2}^{\mathsf{calc}}}{T_{1/2}^{\mathsf{exper}}}$
						τ_e[a]	τ_c[b]	
Black squares plotted in	Fig. 3	^{158}Lu $\rightarrow$ ^{154}Tm	4.81752	0	172.184	−4.433	−3.880	3.6
		^{149}Tb^{m} $\rightarrow$ ^{145}Eu	4.13774	3	175.534	−1.444	−3.096	0.02
		^{154}Ho $\rightarrow$ ^{150}Tb	4.06664	0	179.130	−0.929	−2.254	0.05
		^{154}Ho^{m} $\rightarrow$ ^{150}Tb^{m}	3.84864	2	185.687	−0.230	−0.720	0.32
		^{158}Yb $\rightarrow$ ^{154}Er	4.19734	0	188.434	−0.870	−0.075	6.2
		^{157}Tm $\rightarrow$ ^{153}Ho^{m}	3.83512	0	197.494	−0.036	2.047	121
		^{156}Er $\rightarrow$ ^{152}Dy	3.50709	0	206.217	2.490	4.090	40
		^{150}Gd $\rightarrow$ ^{146}Sm	2.83082	0	218.468	6.253	6.959	5
		^{154}Dy $\rightarrow$ ^{150}Gd	2.96969	0	221.232	6.477	7.606	13
		^{151}Gd $\rightarrow$ ^{147}Sm	2.67564	0	226.275	7.627	8.788	14.5
	Fig. 4	^{157}Lu^{m} $\rightarrow$ ^{153}Tm	5.15627	0	162.254	−5.705	−4.881	6.7

[a] Data taken from Refs. [9, 10].

[b] Calculated values in the present work.

Table 3 - Data regarding α-decay half-lives of Samarium isotopes ($Z = 62$).

		calculated, $\tau_{\mathsf{c}} = \log T^{\mathsf{c}}_{1/2}$ [a]				
Mass Number	Q_α-value	Duarte *et al.*	Denisov	Ren *et al.*	This work	experimental,
A	(MeV)	Ref. [16]	Ref. [17]	Ref. [18]		$\tau_{\mathsf{e}} = \log T^{\mathsf{e}}_{1/2}$ [a]
146	2.55108	8.301	7.941	7.927	8.015	8.017
147	2.33365	11.191	12.401	10.963	11.046	11.028
148	2.00935	16.381	16.031	16.054	16.276	15.806
149	1.89349	18.551	20.071	18.158	18.262	——
150	1.67270	——	28.051	22.652	21.778	——

Figure Captions

Fig. 1 Experimental α-decay half-life values ($T^{\alpha}_{1/2}$ in log scale) plotted against the quantity $(Z-2)^2/[Q_\alpha \cdot (A-4)^{1/3}]$ for lanthanide isotopes. Some α-emitter nuclides are identified near the data-points. The figure displays fifty cases of α-transitions extending for twenty-eight orders of magnitude in $T^{\alpha}_{1/2}$, showing a monotonically increasing behavior (gray line, only to guide the eyes). Experimental data are from Refs. [9, 10].

Fig. 2 Illustrating the variation of the half-life with the area between the total potential-barrier curve $[V(s), a \leq s \leq b]$ and the Q-value (shaded region), for α-transitions of three lanthanide isotopes. The darkest region $(a-c)$ emphasizes the overlapping barrier region where the alpha particle is being formed. The separation barrier $(c-b)$ comprises the Coulomb plus centrifugal (whenever $\ell \neq 0$) contributions to total potential barrier.

Fig. 3 Alpha-decay half-life values, $\tau = \log_{10} T^{\alpha}_{1/2}[a]$ (up to $4.6 \times 10^{18}\, a$), plotted against the total area of the overlapping plus separation barrier regions, $\mathcal{A}_{\rm T}$, limited by the potential energy curves and Q-values for the alpha-transition cases (see Fig. 2). Black circles represent nineteen experimental data of lanthanide isotopes identified by numbers near the points. The straight line results from the weighted least squares fit of these points. The red square highlights the half-life of ^{146}Sm isotope obtained this way. Black squares indicate experimental data that were disregarded in four sequential runs to better fitting. These last cases are listed in Table 2. Half-life data where taken from Refs. [9, 10].

Fig. 4 The same as in Fig. 3 where, here, black triangles represent twenty measured half-life values down to 80 ms. The linear weighted least squares analysis was used to better fit the data. Only one case (black square, listed in Table 2) was disregarded in the analysis.

Fig. 5 Intercomparison between the distributions of $\Delta\tau = \tau_{\mathsf{c}} - \tau_{\mathsf{e}}$ (normalized to 1) from three-decay half-life evaluation procedures for lanthanide isotopes: Deng *et al.* (2020) [21], 50 cases (blue histogram); Zhu *et al.* (2024) [10], 49 cases (red histogram); this work, 40 cases of $|\Delta\tau| \leq 0.48$ (histogram delimiting the grey-shaded region).

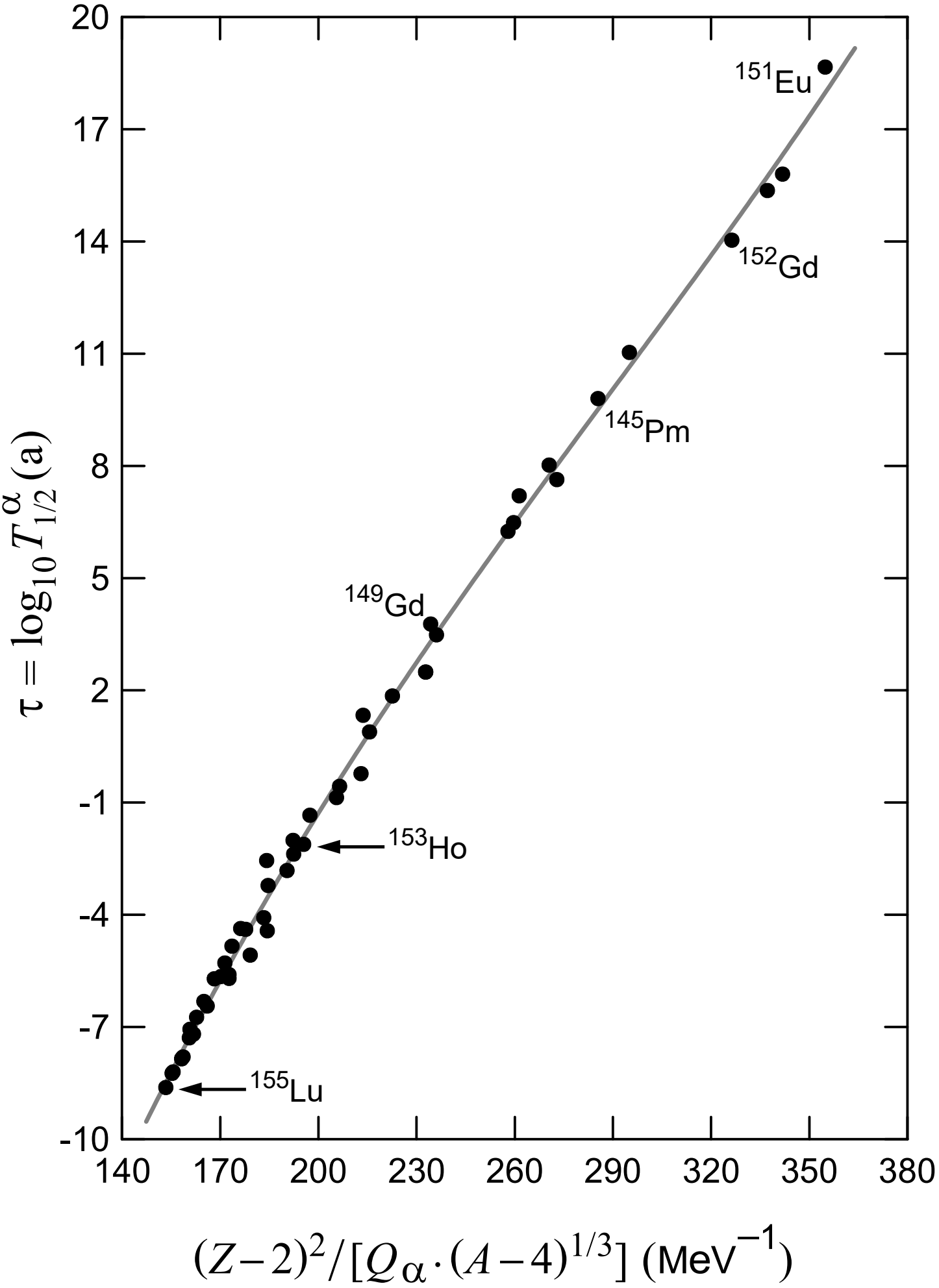
20
17
14
11
8
5
2
-1
-4
-7
-10
140
170
200
230
260
290
320
350
380
$\tau = \log_{10} T^{\alpha}_{1/2}$(a)
$(Z-2)^2/[Q_\alpha \cdot (A-4)^{1/3}]$ (MeV^{-1})
^{151}Eu
^{152}Gd
^{145}Pm
^{149}Gd
^{153}Ho
^{155}Lu

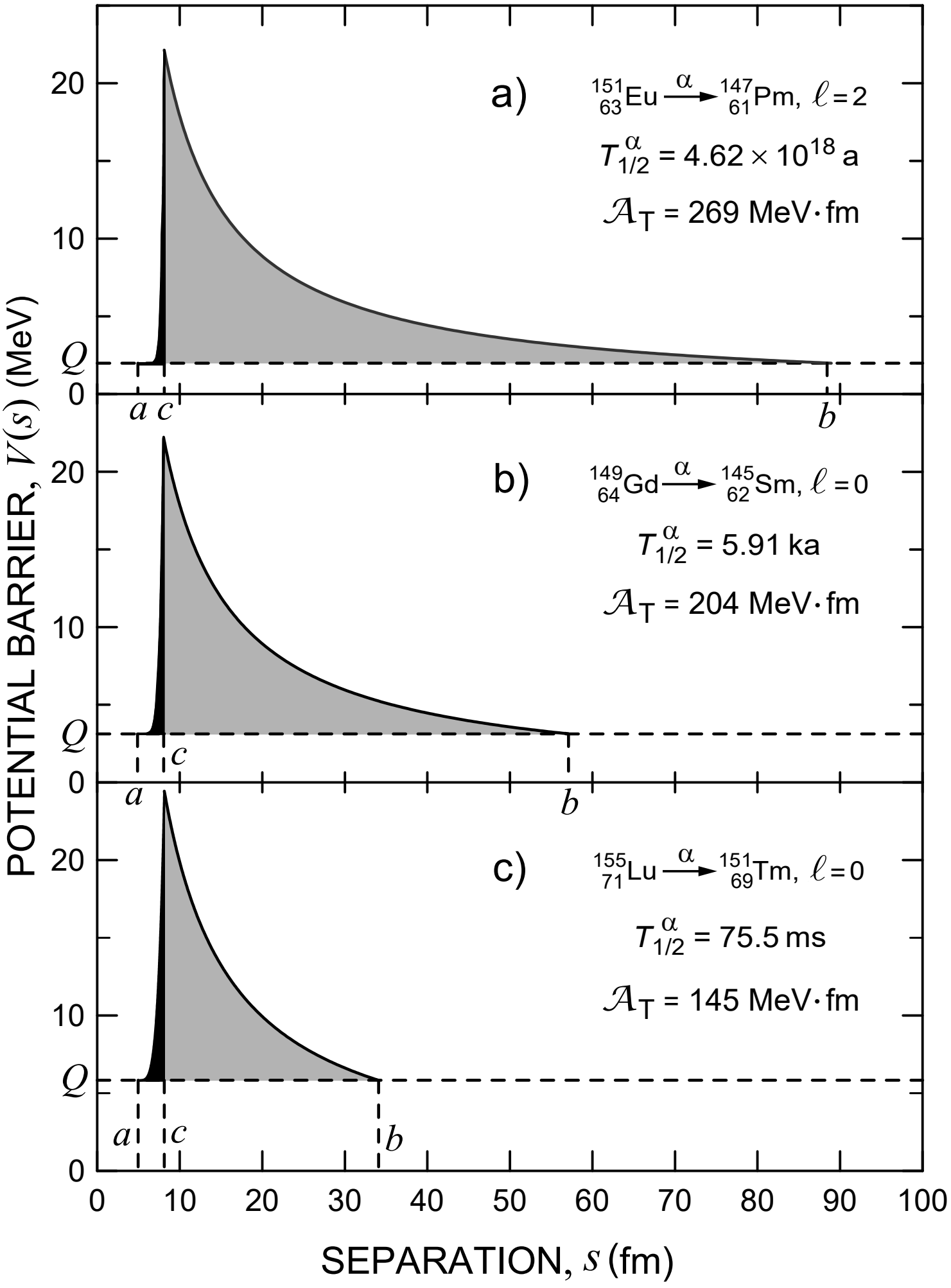
a)
$^{151}_{63}\mathrm{Eu} \xrightarrow{\alpha} {}^{147}_{61}\mathrm{Pm}$, $\ell = 2$
$T^{\alpha}_{1/2} = 4.62 \times 10^{18}$ a
$\mathcal{A}_T = 269$ MeV·fm
b)
$^{149}_{64}\mathrm{Gd} \xrightarrow{\alpha} {}^{145}_{62}\mathrm{Sm}$, $\ell = 0$
$T^{\alpha}_{1/2} = 5.91$ ka
$\mathcal{A}_T = 204$ MeV·fm
c)
$^{155}_{71}\mathrm{Lu} \xrightarrow{\alpha} {}^{151}_{69}\mathrm{Tm}$, $\ell = 0$
$T^{\alpha}_{1/2} = 75.5$ ms
$\mathcal{A}_T = 145$ MeV·fm
POTENTIAL BARRIER, $V(s)$ (MeV)
SEPARATION, s (fm)
Q
a
c
b
0
10
20
30
40
50
60
70
80
90
100

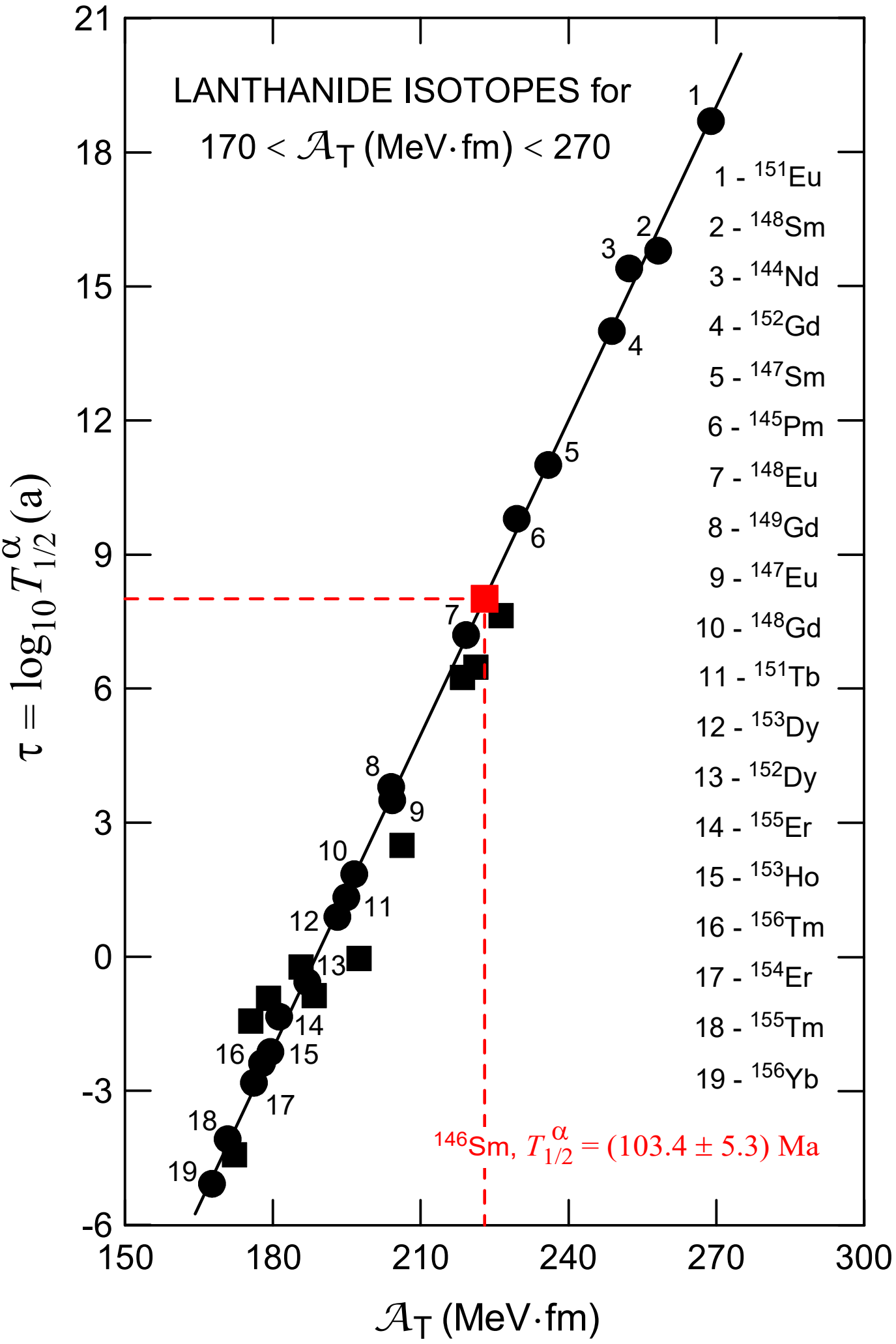
LANTHANIDE ISOTOPES for
170 < $\mathcal{A}_T$ (MeV·fm) < 270
1 - ^{151}Eu
2 - ^{148}Sm
3 - ^{144}Nd
4 - ^{152}Gd
5 - ^{147}Sm
6 - ^{145}Pm
7 - ^{148}Eu
8 - ^{149}Gd
9 - ^{147}Eu
10 - ^{148}Gd
11 - ^{151}Tb
12 - ^{153}Dy
13 - ^{152}Dy
14 - ^{155}Er
15 - ^{153}Ho
16 - ^{156}Tm
17 - ^{154}Er
18 - ^{155}Tm
19 - ^{156}Yb
^{146}Sm, $T_{1/2}^{\alpha} = (103.4 \pm 5.3)$ Ma
$\tau = \log_{10} T_{1/2}^{\alpha}$ (a)
$\mathcal{A}_T$ (MeV·fm)
21
18
15
12
9
6
3
0
-3
-6
150
180
210
240
270
300

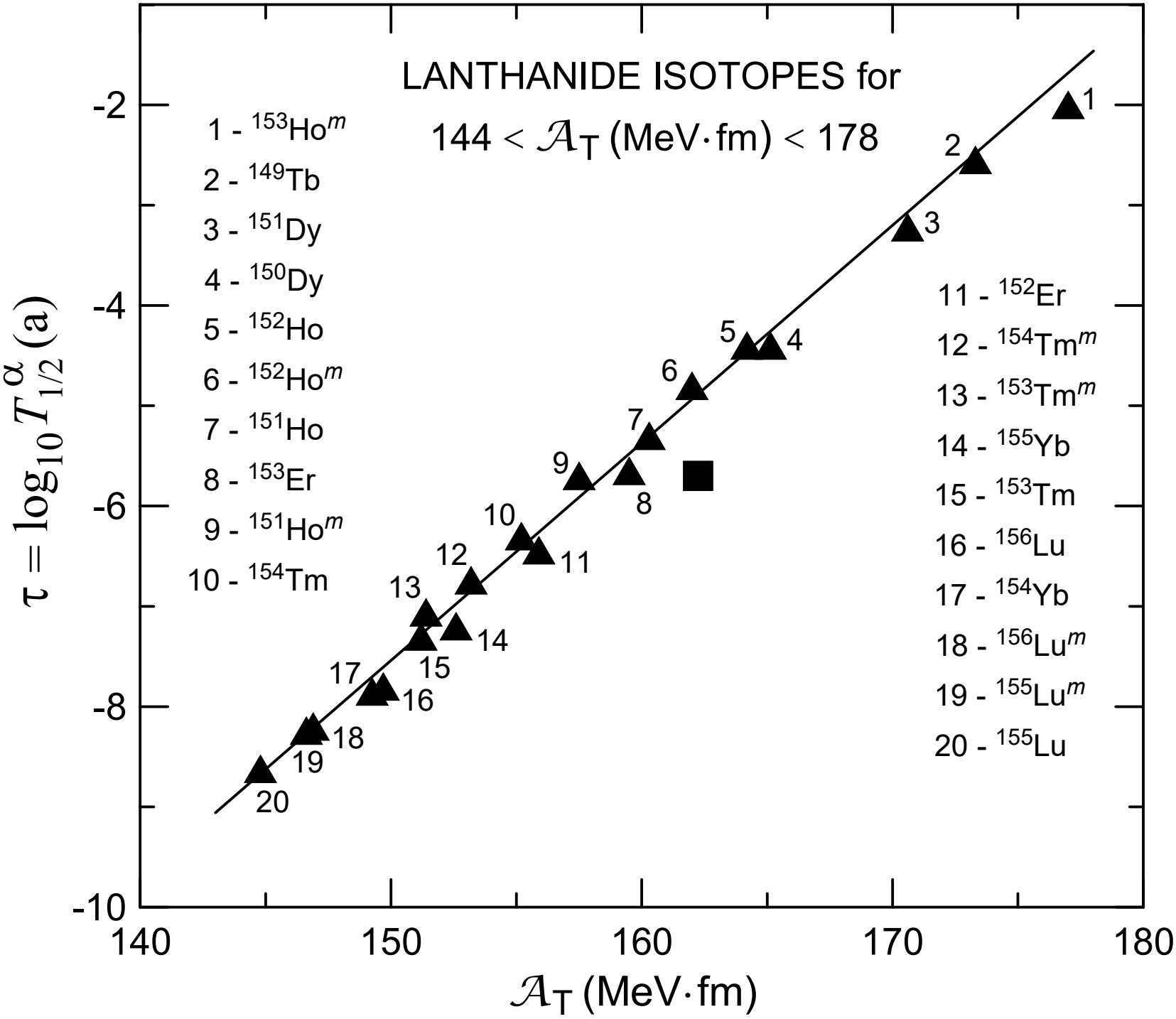
LANTHANIDE ISOTOPES for
144 < $\mathcal{A}_T$ (MeV·fm) < 178
1 - ^{153}Ho^m
2 - ^{149}Tb
3 - ^{151}Dy
4 - ^{150}Dy
5 - ^{152}Ho
6 - ^{152}Ho^m
7 - ^{151}Ho
8 - ^{153}Er
9 - ^{151}Ho^m
10 - ^{154}Tm
11 - ^{152}Er
12 - ^{154}Tm^m
13 - ^{153}Tm^m
14 - ^{155}Yb
15 - ^{153}Tm
16 - ^{156}Lu
17 - ^{154}Yb
18 - ^{156}Lu^m
19 - ^{155}Lu^m
20 - ^{155}Lu
$\tau = \log_{10} T^{\alpha}_{1/2}(a)$
$\mathcal{A}_T$ (MeV·fm)
-2
-4
-6
-8
-10
140
150
160
170
180

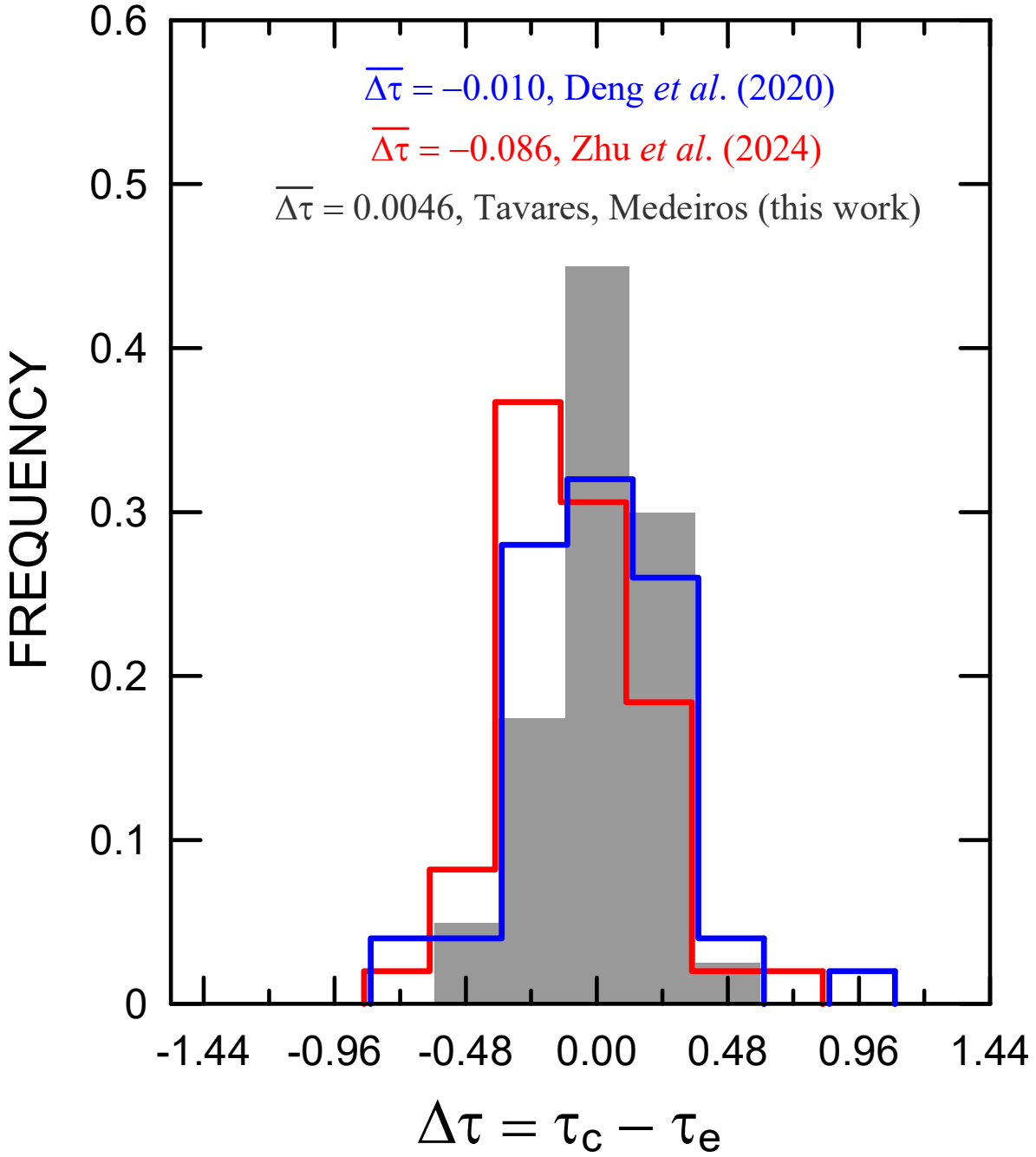
$\overline{\Delta\tau}$ = –0.010, Deng *et al.* (2020)
$\overline{\Delta\tau}$ = –0.086, Zhu *et al.* (2024)
$\overline{\Delta\tau}$ = 0.0046, Tavares, Medeiros (this work)
FREQUENCY
0.6
0.5
0.4
0.3
0.2
0.1
0
-1.44
-0.96
-0.48
0.00
0.48
0.96
1.44
$\Delta\tau = \tau_c - \tau_e$

NOTAS DE FÍSICA é uma pré-publicação de trabalho original em Física.
Pedidos de cópias desta publicação devem ser enviados aos autores ou ao:

Centro Brasileiro de Pesquisas Físicas
Área de Publicações
Rua Dr. Xavier Sigaud, 150 – 4º andar
22290-180 – Rio de Janeiro, RJ
Brasil
E-mail: alinecd@cbpf.br/valeria@cbpf.br
http://portal.cbpf.br/publicacoes-do-cbpf

NOTAS DE FÍSICA is a preprint of original unpublished works in Physics.
Requests for copies of these reports should be addressed to:

Centro Brasileiro de Pesquisas Físicas
Área de Publicações
Rua Dr. Xavier Sigaud, 150 – 4º andar
22290-180 – Rio de Janeiro, RJ
Brazil
E-mail: alinecd@cbpf.br/valeria@cbpf.br
http://portal.cbpf.br/publicacoes-do-cbpf